Electronic supporting information

A role for low concentration reaction intermediates in the signal amplification by reversible exchange process revealed by theory and experiment

Marianna Fekete,[a] Soumya S. Roy[a,b] and Simon B. Duckett[a]

[a] *Centre for Hyperpolarization in Magnetic Resonance, University of York, Heslington, York, YO10 5NY, UK*

[b] *Department of Inorganic and Physical Chemistry, Indian Institute of Science, Bangalore 560012, India.*

Contents

General Procedure for the preparation of NMR samples for SABRE analysis

SABRE measurements were conducted in either a 5 mm NMR tube fitted with a Young's valve (Method 1) or an automated polarizer (Method 2).

Method 1

NMR samples were prepared in 5 mm NMR tubes fitted with Young's valves. Samples were degassed three times on a high vacuum Schlenk line whilst immersing the solution in a dry CO_2/acetone slush bath prior to *p*-H_2 (3 bar) addition. In a typical experiment, the iridium complex, [IrCl(NHC)(COD)] (5.2 mM, NHC = Cl-IPhMe$_2$, IMes and d_{16}-Cl-IPhMe$_2$, d_{22}-IMes) and seven equivalents of the substrate (nicotinamide (**NA**), methyl-nicotinate (**MN**), pyridine) based in iridium were dissolved in methanol-d_4 (0.6 ml). The mixture was degassed and *para*hydrogen at a pressure of 3 bar was added. When the samples were analysed, samples were shaken for 10 s at 65 G before rapidly transporting them into the magnet for the final NMR measurement. We note that we use different catalysts in these experiments for the two substrates as NHC Cl-IPhMe$_2$ is better suited for **NA** whilst d_{22}-IMes is superior for **MN**.

Method 2

An automated polarizer method was used to analyse a mixture containing [IrCl(NHC)(COD)] (5.2 mM) and seven equivalents of the corresponding substrate in d_4-methanol (3 mL). The automated device has been described previously.[1] The solvent, catalyst and substrate were placed in a glass tube with two side arms (the mixing chamber) and this is where the hyperpolarization transfer step takes place. To enable variable temperature measurements to be made, the previously described mixing chamber was modified to include a water jacket that was linked to a constant temperature bath (Fig. S1). The mixing chamber was then surrounded by a copper coil that could be used to apply a 0-140 G magnetic field. All magnitudes of the magnetic field in which the polarization transfer step occurs are stated without correction for the local earth's field of around 0.5 G. The operation of this system is entirely automated - the liquid and gas flow from the mixing chamber is

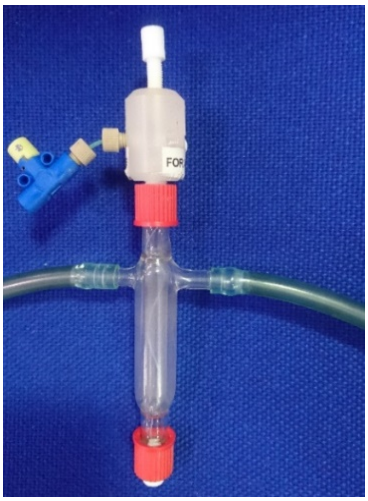

Fig. S1. Mixing chamber with water jacket used in this study

computer controlled *via* the NMR pulse program. The mixing chamber was cooled or heated by solvent flow from an external circulating water pump whose solution was set to have a specified temperature between 278 and 313 K. *Para*hydrogen was introduced continuously from an external *para*hydrogen (*para*-H_2) generator into the mixing chamber to activate the catalyst. Nitrogen gas was then used to transfer the hyperpolarized solution from the mixing chamber into the NMR probe head for measurement. Before taking a ^{1}H NMR measurement, the *para*hydrogen bubbling time was set to 6 s. The transportation time of this solution into the NMR probe was calibrated as 0.4 s. A further delay of 0.5 s was introduced to allow for sample settling prior to signal acquisition.

Method used to calculate the reported ^{1}H NMR enhancement factors

The ^{1}H NMR signal enhancement was calculated according to the following equation:

$$\textbf{\textit{signal enhancement}} = \frac{\textbf{\textit{signal of polarized sample measured by integral}}}{\textbf{\textit{signal of unpolarized sample measured by integral}}}$$

The reference spectrum (spectrum of the unpolarised sample) was measured on the same sample after its NMR response was fully relaxed. The reference spectrum and the hyperpolarized spectrum were measured using the same acquisition, delay and receiver gain parameters. The raw integrals of the relevant resonances in the reference and the hyperpolarized spectra were used to determine the enhancement levels using the equation above. The results are not corrected for relaxation losses during the transfer time (0.9 s for flow measurements and *ca.* 4 s for NMR tube measurements) into the NMR magnet and hence reflect experimentally observed values.

Flow experiments with nicotinamide

The summed intensity profiles for the ^{1}H NMR signals of protio nicotinamide at 296 and 303 K as a function of magnetic field over the range 0.5 mG to 140 G were determined (Fig. S2). The profile shows a simple maxima centred on 70 G. These data result from taking the precatalyst [IrCl(COD)(Cl-IPhMe$_2$)] (5.2 mM) (Cl-IPhMe$_2$= 1,3-bis(4-chloro-2,6-dimethylphenyl)imidazole-2-ylidine))[2] and reacting it with seven equivalent of nicotinamide (**NA**) in d_4-methanol solution (3 mL) under 3 bar of *para*-H_2.

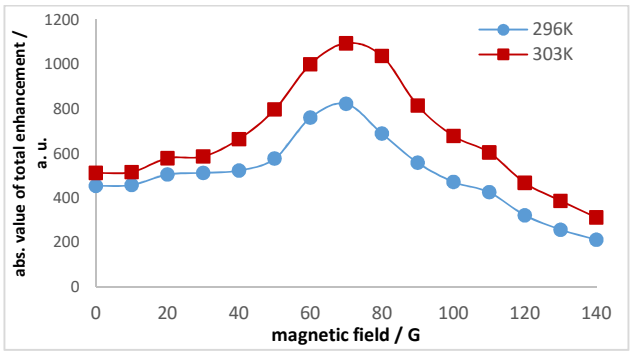

Fig. S2: Absolute values of total ^{1}H NMR signal gains for **NA** at the specified temperature as a function of PTF

Flow experiments with d_2-4,6-nicotinamide

The summed intensity profiles for the ^{1}H NMR signals of d_2-4,6-nicotinamide (***d*$_2$-NA**) at 296 and 303 K as a function of magnetic field over the range 0.5 mG to 140 G are presented in Fig. S3. This is achieved by taking the precatalyst [IrCl(COD)(Cl-IPhMe$_2$)] (5.2 mM) and reacting it with seven equivalents of d_2-4,6-nicotinamide (***d*$_2$-NA**) based on iridium in d_4-methanol solution (3 mL) under 3 bar of *para*-H_2.

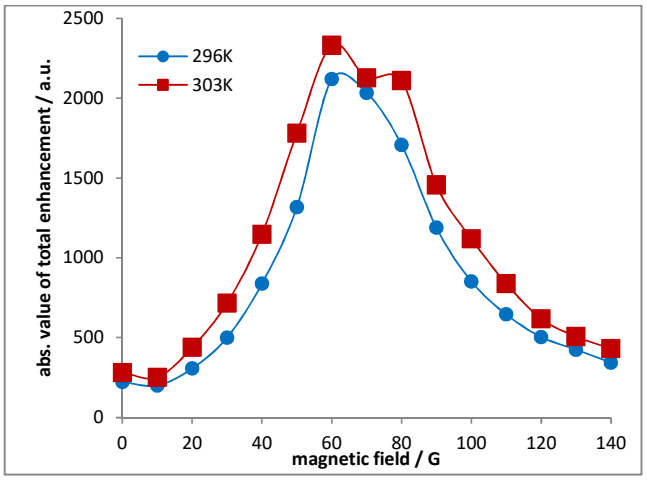

Fig. S3: Total ^{1}H NMR signal gains for ***d*$_2$-NA** at the specified temperature as a function of PTF.

Flow experiments with d_{16}-Cl-IPhMe$_2$ and d_2-4,6-nicotinamide

The summed intensity profiles for the ^{1}H NMR signals of d_2-4,6-nicotinamide between 296 and 303 K as a function of magnetic field over the range 0.5 mG to 140 G. This is achieved here by taking the precatalyst [IrCl(COD)(d_{16}-Cl-IPhMe$_2$)] (5.2 mM) and reacting it with seven equivalent of d_2-4,6-nicotinamide (***d*$_2$-NA**) in d_4-methanol solution (3 mL) under 3 bar of *para*-H$_2$. The data resulting is presented in Fig. S4.

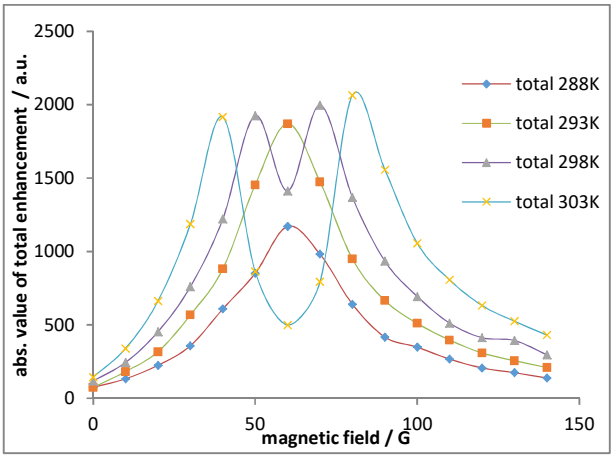

Fig. S4: Total ^{1}H NMR signal gains for ***d*$_2$-NA** at the specified temperature as a function of PTF using precatalyst [IrCl(COD)(d_{16}-Cl-IPhMe$_2$)].

Flow experiments with d_2-4,6-nicotinamide in the presence of NCMe

The summed intensity profiles for the ^{1}H NMR signals of d_2-4,6-nicotinamide at 296 and 303 K as a function of magnetic field over the range 0.5 mG to 140 G. This is achieved by taking the precatalyst [IrCl(COD)(Cl-IPhMe$_2$)] (5.2 mM) and reacting it with seven equivalents of d_2-4,6-nicotinamide (***d*$_2$-NA**) in d_4-methanol solution (3 mL) with 1.3 equivalents of CH_3CN under 3 bar of *para*-H$_2$. The data resulting is presented in Fig. S5.

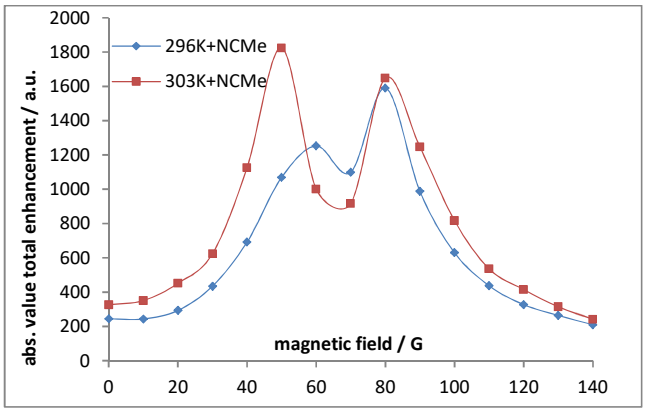

Fig. S5: Total ^{1}H NMR signal gains for ***d*$_2$-NA** at the specified temperature as a function of PTF using precatalyst [IrCl(COD)(Cl-IPhMe$_2$)] with CH_3CN present.

Signals visible in the hydride region of the ^{1}H NMR spectra of the 5.2 mM d_4-methanol solution with the precatalyst [IrCl(COD)(Cl-IPhMe$_2$)] and a 7-fold nicotinamide in the presence of *para*-H_2 are shown in Fig. S6 with NCMe (1.3-fold, above) and without (below).

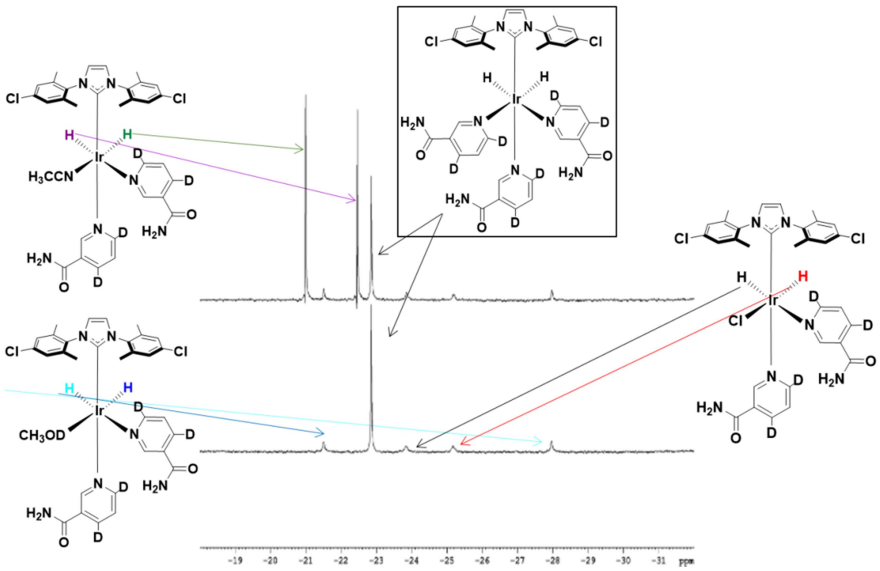

Fig. S6. ^{1}H NMR spectra showing the hydride region of samples of precatalyst [IrCl(COD)(Cl-IPhMe$_2$)] (5.2 mM) with seven equivalents of d_2-4,6-nicotinamide (***d*$_2$-NA**) in d_4-methanol solution (3 mL) under 3 bar of *para*-H_2. Upper with CH_3CN (this solution yields the results associated with Fig. S5), below without CH_3CN.

Flow experiments with d_{16}-Cl-IPhMe$_2$, d_2-4,6-nicotinamide and NCMe

The summed intensity profiles for the ^{1}H NMR signals of d_2-4,6-nicotinamide at 296 and 303 K as a function of magnetic field over the range 0.5 mG to 140 G (Fig. S7). This is achieved by taking the precatalyst [IrCl(COD)(d_{16}-Cl-IPhMe$_2$)] (5.2 mM) and reacting it with seven equivalents of d_2-4,6-nicotinamide (***d*$_2$-NA**) in d_4-methanol solution (3 mL) under 3 bar of *para*-H_2 in the presence of 1.3 equivalents of CH_3CN.

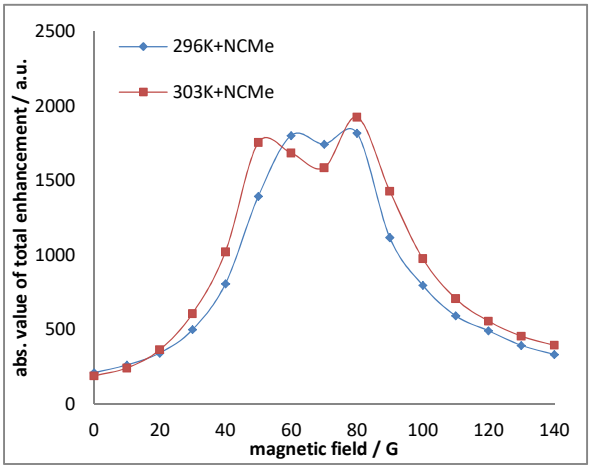

Fig. S7: Total ^{1}H NMR signal gains for ***d*$_2$-NA** at the specified temperature as a function of PTF using precatalyst [IrCl(COD)(d_{16}-Cl-IPhMe$_2$)] with CH_3CN present.

Graphical analysis of the experimentally observed signal intensity

From a graphical perspective, the change in experimental signal intensity behaviour with temperature in methanol solution can be recreated approximately if plots with a single maximum based on the action of [Ir(H)$_2$(NHC)(***d*$_2$-NA)$_3$]Cl are added to one with two maxima that are centre at 50 and 80 and based on the action of [Ir(H)$_2$(NHC)(***d*$_2$-NA)$_2$(CH_3CN)]Cl. These data aim therefore to demonstrate a role for either Ir(H)$_2$(NHC)(***d*$_2$-NA)$_2$Cl or [Ir(H)$_2$(NHC)(***d*$_2$-NA)$_2$(MeOH)]Cl in the more general SABRE PTF profiles. Fig. S8a shows data for the ^{1}H NMR signal gain associated with the *ortho* proton resonances of ***d*$_2$-NA** at 303 K, with and without the co-ligand acetonitrile. Fig. 8b shows the impact of adding these two traces together with a 50:50 weighting. The result matches the appearance of Fig. S4. If this ratio is changed to a 20:80 weighting, Fig. S8c results. There is now a much larger dip which is reflected in the experimental results at higher temperatures (see Fig. 2).

Filed/ G	303K+NCMe	303K
0	172.247	142.2417
10	185.3918	128.1438
20	235.2587	216.6823
30	321.5717	344.844
40	567.7007	545.672
50	903.3354	842.9055
60	568.1282	1100.301
70	372.796	1100.286
80	814.5137	992.8347
90	620.7886	685.4882
100	410.8583	530.1418
110	271.5013	399.2019
120	210.87	293.3229
130	159.7204	241.3957
140	123.4747	205.9564

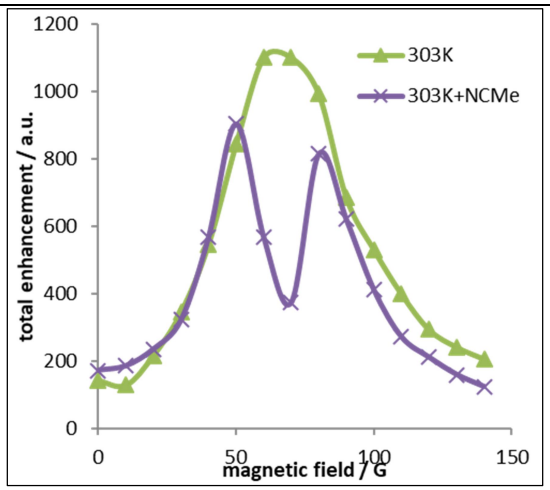

Filed/ G	303K+NCMe	303K	Sum (0.5 : 0.5)
0	172.247	142.2417	157.2444
10	185.3918	128.1438	156.7678
20	235.2587	216.6823	225.9705
30	321.5717	344.844	333.2079
40	567.7007	545.672	556.6864
50	903.3354	842.9055	873.1205
60	568.1282	1100.301	834.2147
70	372.796	1100.286	736.5408
80	814.5137	992.8347	903.6742
90	620.7886	685.4882	653.1384
100	410.8583	530.1418	470.5001
110	271.5013	399.2019	335.3516
120	210.87	293.3229	252.0965
130	159.7204	241.3957	200.5581
140	123.4747	205.9564	164.7156

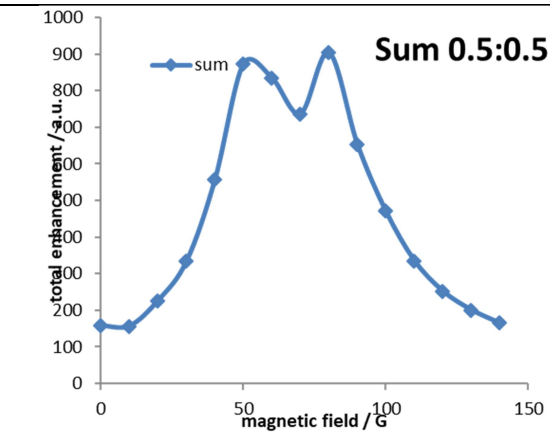

Filed/ G	303K+NCMe	303K	Sum (0.8 : 0.2)
0	172.247	142.2417	166.2459
10	185.3918	128.1438	173.9422
20	235.2587	216.6823	231.5434
30	321.5717	344.844	326.2262
40	567.7007	545.672	563.295
50	903.3354	842.9055	891.2494
60	568.1282	1100.301	674.5628
70	372.796	1100.286	518.2939
80	814.5137	992.8347	850.1779
90	620.7886	685.4882	633.7285
100	410.8583	530.1418	434.715
110	271.5013	399.2019	297.0414
120	210.87	293.3229	227.3606
130	159.7204	241.3957	176.0555
140	123.4747	205.9564	139.971

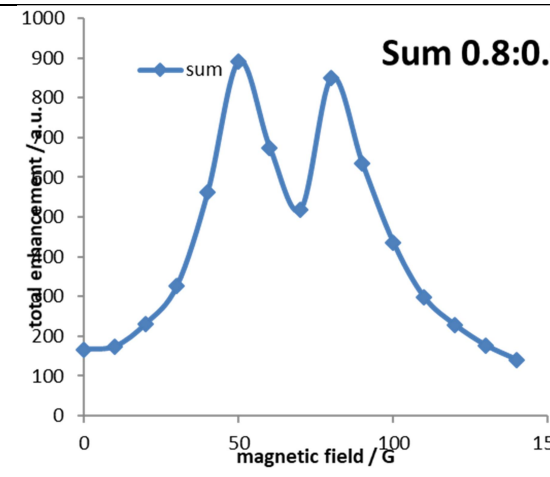

Fig. S8: Impact of catalyst speciation on the PTF profiles for the ^{1}H NMR signal gains of the *ortho* proton resonances of d_2-4,6-nicotinamide. (a) Based on the action of $[Ir(H)_2(NHC)(\boldsymbol{d_2}\text{-NA})_3]Cl$ or $[Ir(H)_2(NHC)(\boldsymbol{d_2}\text{-NA})_2(CH_3CN)]Cl$ as indicated. (b) Summation of the results of Fig. S8a with a 50:50 weighting. (c) Summation of the results of Fig. S8a with a 20:80 weighting

Flow experiments with pyridine

The summed intensity profiles for the ^{1}H NMR signal gains of pyridine at temperature range from 278 K to 308 K at a function of magnetic field over the range 0.5 mG to 140 G (Fig. S9). The experimental data This is achieved by taking the precatalyst [IrCl(COD)(IMes)] (5.2 mM) and reacting it with seven equivalents of pyridine in d_4-methanol solution (3 mL) under 3 bar of *para*-H_2.

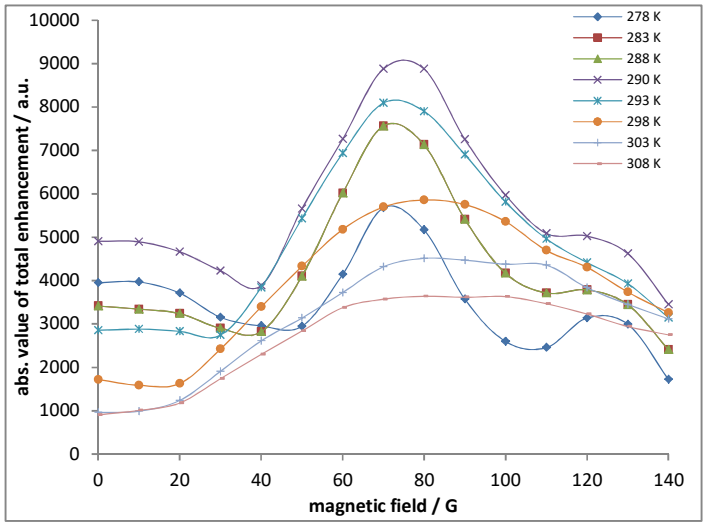

Fig. S9: Total ^{1}H NMR signal gains for pyridine at the specified temperature as a function of PTF using precatalyst [IrCl(COD)(IMes)].

Dissociation rates for pyridine

Table S1: Observed dissociation rates for pyridine in 5.2 mM d_4-methanol solution of [IrCl(COD)(IMes)] in conjunction with a 7-fold excess of pyridine based on iridium (leads to 4-fold excess in solution when the active catalyst is formed) under 3 bar of *para*-H_2.

Temperature / K	exchange rate / s^{-1}
278	**1.01**
283	**2.22**
288	**4.33**
290	**5.42**
293	**7.51**
298	**13.3**
303	**28.5**

Theoretical calculations

The method of Green was used to create a theoretical basis to the PTF data reported in this work.[3] The matrix elements used to simulate the PTF plots for ***d*$_2$-NA** are listed in Tables S2 and S3. The labels 1 and 2 represent H2 and H5 of this substrate, whilst 3 and 4 signify the hydride protons in complexes of type **A** or **B**. The chemical shifts of these protons are shown in the diagonal elements of the matrix according to a ppm scale,

whereas typical values of the J-couplings between these groups are shown as off-diagonal elements and have Hz as their units.

Table S2: Data used to simulate the PTF behaviour of d_2-nicotinamide (***d*$_2$-NA**) via a catalyst of the type [Ir(H)$_2$(Cl-IPhMe$_2$)(***d*$_2$-NA**)$_3$]Cl (Type B).

	1	**2**	**3**	**4**
1	9.10			
2	0.7	7.40		
3	0.1	0.1	-21.8	
4	0.01	0.7	-7.7	-21.8

Table S3: Data used to simulate the PTF behaviour of d_2-nicotinamide (***d*$_2$-NA**) via a catalyst of the type [Ir(H)$_2$(Cl-IPhMe$_2$)(***d*$_2$-NA**)$_2$(CD$_3$CN)]Cl (Type A).

	1	**2**	**3**	**4**
1	9.10			
2	0.7	7.40		
3	0.1	0.1	-22.18	
4	0.01	0.7	-7.7	-20.65

The values of these couplings were varied systemically to probe there effect on the PTF plots as detailed in the manuscript. These effects are described in Figure 1 of the manuscript for the situation wherein the hydrides are inequivalent. Fig. S10 portrays the same results for situation B where the hydrides are now chemically identical but magnetically distinct. As the results demonstrate, essentially identical behaviour is evident. We predict that the related chloride and methanol adducts will behave in a similar way. Hence the involvement of these two catalysts can readily be distinguished from one another by virtue of variations in the corresponding PTF plots.

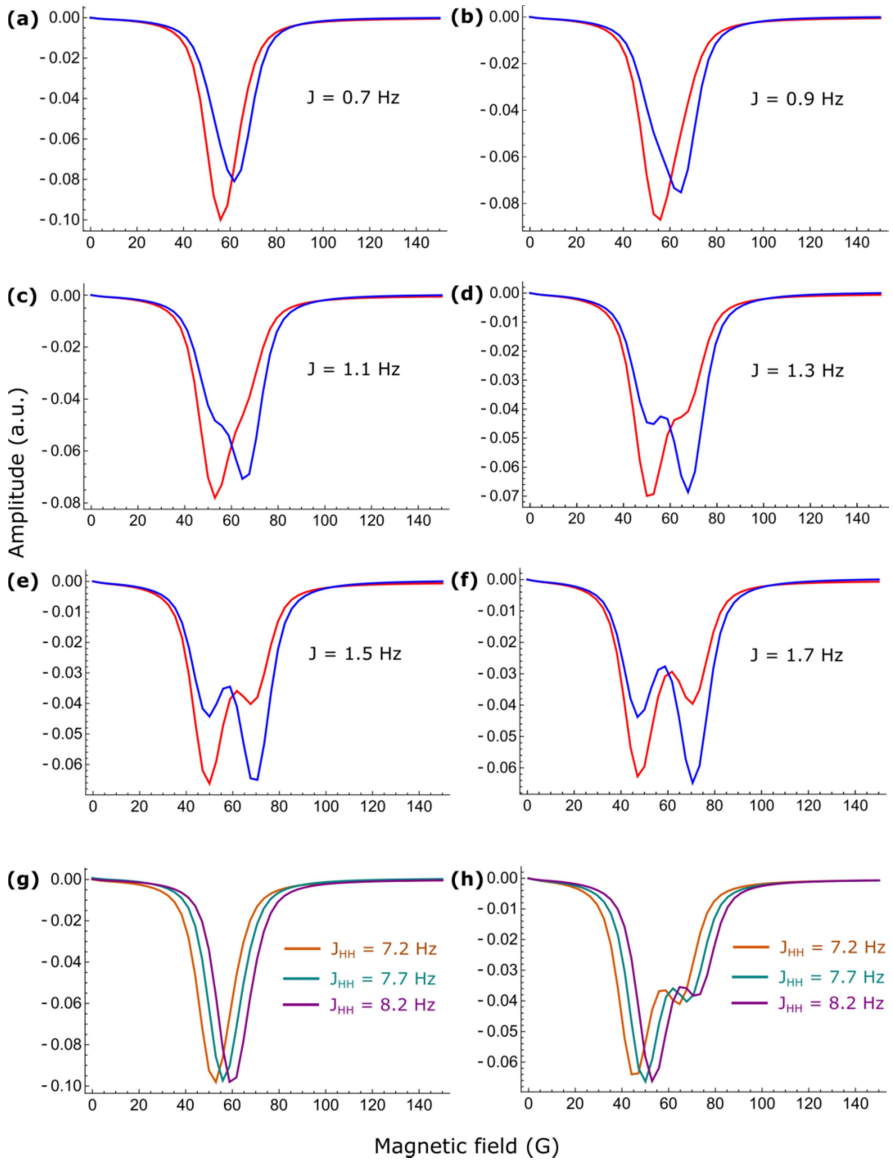

Fig. S10 (a)-(f) Theoretically predicted ^{1}H NMR SABRE signal gain profiles as a function of polarisation transfer field (PTF) for the substrate d_2-4,6-nicotinamide. The six plots detailing the *ortho* proton H2 (red) and *meta* proton (H5, blue) responses were produced by the action of a type **B** catalyst of Scheme 1 and involve the use of the listed interproton couplings between H2 and H5. The hydride-hydride coupling was set to 7.7 Hz, and the *trans*-hydride-H2 coupling 0.7 Hz. Plots (g) and (h) illustrate the effect the hydride-hydride coupling plays on the *ortho* H2 proton PTF profile for the situation when hydride-H2 coupling is 0.7 Hz and the H2-H5 coupling is 0.9 and 1.5 Hz respectively.

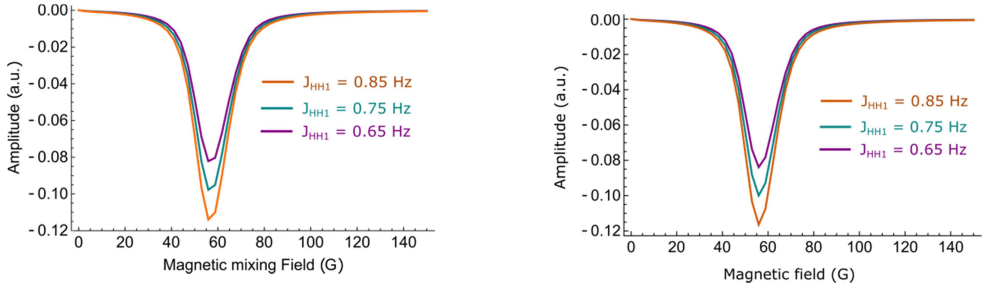

Fig. S11 Theoretically predicted ^{1}H NMR SABRE signal gain profiles as a function of polarisation transfer field (PTF) for the substrate d_2-4,6-nicotinamide. The plots detail the *ortho* proton H2 response and were produced by the action of a type **A** catalyst (left) and **B** catalyst (right) of Scheme 1 and involve use of the listed *trans* hydride proton H2 couplings. The hydride-hydride coupling was set to 7.7 Hz, and the H2-H5 coupling 0.7 Hz.

Flow experiments with IMes and d_2-4,6-methyl-nicotinate

The summed signal intensity profiles for the ^{1}H NMR signal gains of d_2-4,6-methyl-nicotinate over the temperature range 283 K to 308 K as a function of magnetic field over the range 0.5 mG to 140 G are presented in Fig. S12). In order to collect this data, the precatalyst [IrCl(COD)(IMes)] (5.2 mM) was reacted with seven equivalents of d_2-4,6-methyl-nicotinate (d_2-MN) in d_4-methanol solution (3 mL) under a 3 bar pressure of *para*-H_2. We illustrate here how the PTF is broadened presumably due to couplings into the imidazole.

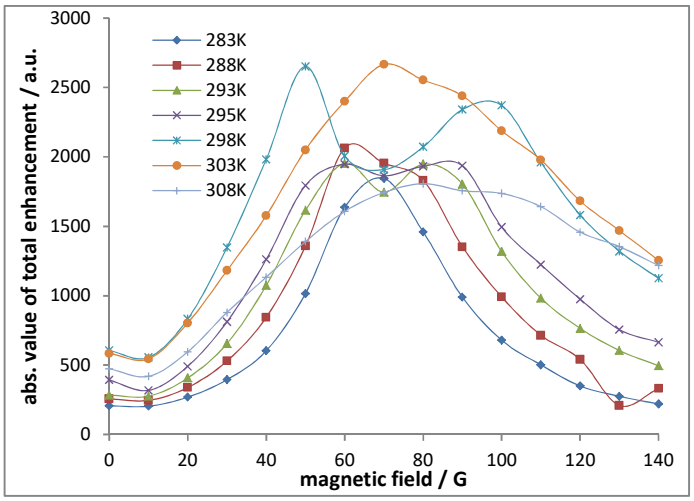

Fig. S12: Total ^{1}H NMR signal gains for d_2-4,6-methyl-nicotinate at the specified temperature as a function of PTF using precatalyst [IrCl(COD)(IMes)]

Flow experiments with d_{22}-IMes and d_2-4,6-methyl-nicotinate

The summed and normalized intensity profiles for the ^{1}H NMR signal gains of d_2-4,6-methyl-nicotinate over the temperature range 283 K and 303 K (as indicated) as a function of magnetic field (0.5 mG to 140 G). These data are collected by taking the precatalyst [IrCl(COD)(d_{22}-IMes)] (5.2 mM) and reacting it with seven equivalents of d_2-4,6-methyl-nicotinate (***d*$_2$-MN**) based on iridium in d_4-methanol solution (3 mL) under 3 bar of *para*-H_2. The resulting data are presented in Fig. S13.

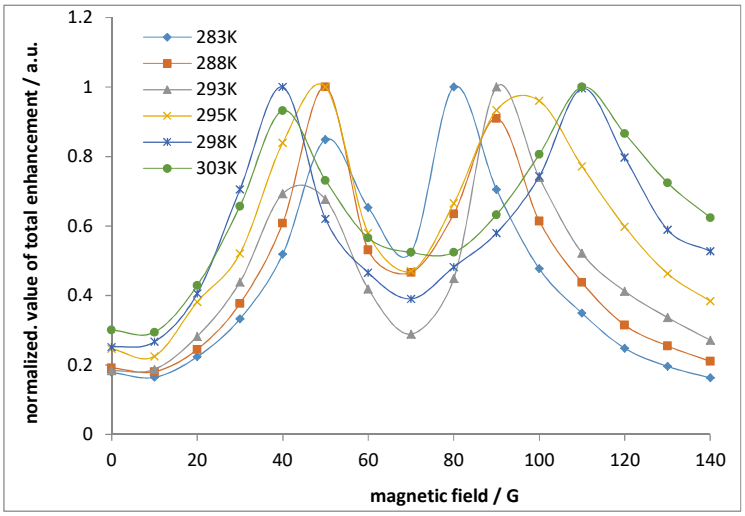

Fig S13: Total ^{1}H NMR signal gains for d_2-4,6-methyl-nicotinate at the specified temperature as a function of PTF using precatalyst [IrCl(COD)(IMes)].

Coupling constant determination for the bound d_2-NA ligand

A series of standard selective one dimensional NMR COSY experiments were recorded to probe the build-up of cross peak intensity under J-coupling transfer as a function of mixing time for H2 and H5 the ***d*$_2$-NA** ligands in [Ir(H)$_2$(d_{16}-Cl-IPhMe$_2$)(***d*$_2$-NA**)$_3$]Cl and [Ir(H)$_2$(d_{16}-Cl-IPhMe$_2$)(***d*$_2$-NA**)$_2$(NCMe)]Cl that lie *trans* to hydride. These results, which were recorded at 263 K to limit ligand exchange, are presented in Figure S14 and S15 respectively. A similar set of data could not be collected on Ir(H)$_2$(Cl-IPhMe$_2$)(***d*$_2$-NA**)$_2$Cl, which forms as the dominant species in dichlormethane-d_2 due to hindered rotation which results in significant broadening of all associated resonances at low temperature. On this basis we suggest that arrangement **A** and **B** of [Ir(H)$_2$(Cl-IPhMe$_2$)(***d*$_2$-NA**)$_2$(NCMe)]Cl) and [Ir(H)$_2$(Cl-IPhMe$_2$)(***d*$_2$-NA**)$_3$]Cl respectively exhibit couplings of 1.38 and 1.17 Hz. We also analysed the corresponding situation in [Ir(H)$_2$(d_{22}-IMes)(***d*$_2$-MN**)$_2$(NCMe)]Cl) and [Ir(H)$_2$(d_{22}-IMes)(***d*$_2$-MN**)$_3$]Cl where we found J_{HH} values of 1.67 and 1.17 Hz respectively. These data are illustrated in Figures S16-S17.

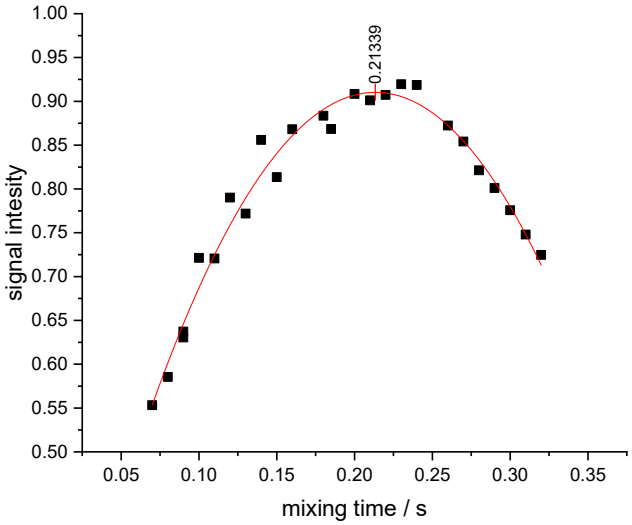

Fig S14: COSY data used to determine the coupling between H2 and H5 in the ***d*$_2$-NA** ligands of [Ir(H)$_2$(Cl-IPhMe$_2$)(***d*$_2$-NA**)$_3$]Cl that lie *trans* to hydride.

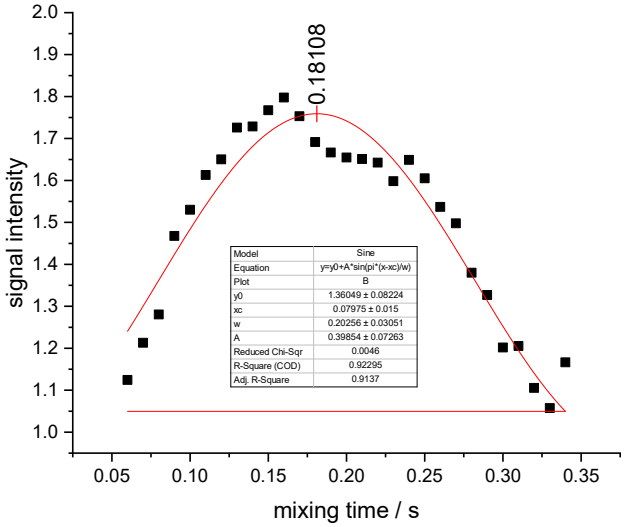

Fig S15: COSY data used to determine the coupling between H2 and H5 in the ***d*$_2$-NA** ligand of [Ir(H)$_2$(Cl-IPhMe$_2$)(***d*$_2$-NA**)$_2$(NCMe)]Cl that lie *trans* to hydride.

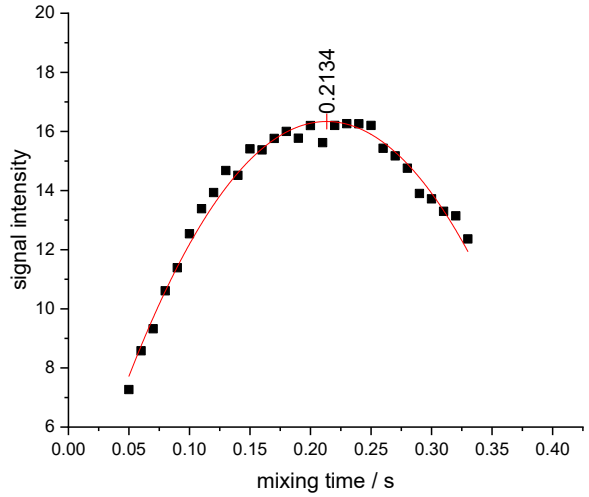

Fig S16: COSY data used to determine the coupling between H2 and H5 in the ***d*$_2$-MN** ligands of [Ir(H)$_2$(*d*$_{22}$-IMes)(***d*$_2$-MN**)$_3$]Cl that lie *trans* to hydride.

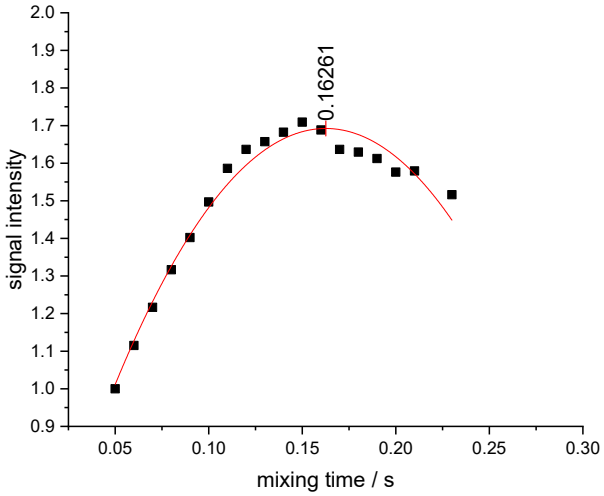

Fig S17: COSY data used to determine the coupling between H2 and H5 in the d_2-MN ligand of [Ir(H)$_2$(*d*$_{22}$-IMes)(***d*$_2$-MN**)$_2$(NCMe)]Cl that lie *trans* to hydride.

References

[1] a) L. S. Lloyd, R. W. Adams, M. Bernstein, S. Coombes, S. B. Duckett, G. G. R. Green, R. J. Lewis, R. E. Mewis and C. J. Sleigh, *Journal of the American Chemical Society* **2012**, *134*, 12904-12907; b) F. Marianna, R. P. J., G. G. G. R. and D. S. B., *Magnetic Resonance in Chemistry* **2017**, *55*, 944-957.
[2] P. J. Rayner, P. Norcott, K. M. Appleby, W. Iali, R. O. John, S. J. Hart, A. C. Whitwood and S. B. Duckett, *Nature Communications* **2018**, *9*, 4251.
[3] R. W. Adams, S. B. Duckett, R. A. Green, D. C. Williamson and G. G. R. Green, *Journal of Chemical Physics* **2009**, *131*.